optica

Stably accessing octave-spanning microresonator frequency combs in the soliton regime: supplementary material

Qing Li[1,3,*], Travis C. Briles[2], Daron A. Westly[1], Tara E. Drake[2], Jordan R. Stone[2], B. Robert Ilic[1], Scott A. Diddams[2], Scott B. Papp[2], and Kartik Srinivasan[1,*]

[1] *Center for Nanoscale Science and Technology, National Institute of Standards and Technology, Gaithersburg, Maryland 20899, USA*
[2] *Time and Frequency Division, National Institute of Standards and Technology, Boulder, Colorado 80305, USA*
[3] *Maryland NanoCenter, University of Maryland, College Park, Maryland 20742, USA*
[*] *Corresponding author: qing.li@nist.gov, kartik.srinivasan@nist.gov*

Published 2 February 2017

This document provides supplementary information to "Stably accessing coherent octave-spanning microresonator frequency combs in the soliton regime," https://doi.org/10.1364/optica.4.000193. It describes the numerical simulation to obtain the thermal properties of the microresonator, and also lists the parameters used in the LLE simulations shown in the main text.

https://doi.org/10.1364/optica.4.000193.s001

1. SIMULATIONS ON THERMAL PARAMETERS

The thermal dynamics in a microresonator are described by the following equation [1, 2]:

$$\frac{dT_{\text{eff}}}{dt} = -\gamma_T \left(T_{\text{eff}} - \frac{P_{\text{abs}}}{K_c} \right), \tag{S1}$$

where γ_T is the thermal decay rate, K_c is the thermal conductance of the microresonator, and P_{abs} denotes the absorbed optical power. T_{eff} is an effective temperature computed by averaging the temperature of the cavity, $T(\mathbf{r}, t)$, over the optical mode volume as

$$T_{\text{eff}} = \frac{\int T(\mathbf{r}, t) n^2(\mathbf{r}) |E(\mathbf{r})|^2 \, d^3\mathbf{r}}{\int n^2(\mathbf{r}) |E(\mathbf{r})|^2 \, d^3\mathbf{r}}, \tag{S2}$$

where $n(\mathbf{r})$ denotes the refractive index and $E(\mathbf{r})$ is the electric field of the cavity mode.

To obtain the numerical values of the the thermal decay rate and the thermal conductance, we implement the heat transfer equation based on the finite element method (FEM) for the resonator structure (See Fig. S1(a)). The heat source is assumed to have the same intensity distribution as the resonant mode (i.e., we assume a linear absorption of optical power). By fitting the simulation results (Fig. S1(b)) with Eq. S1, we obtain $\gamma_T = 2.9 \times 10^5$ Hz and $K_c = 2.86 \times 10^{-4}$ W/K for a 23 μm radius Si_3N_4 microring resonator.

2. PARAMETERS USED IN LLE SIMULATION

In this section, we list the major parameters used in the LLE simulations shown in the main text, including Figs. 4-6 and 8. In Fig. 4, we have adopted similar parameters as used in Ref. [3], where the dispersion of the microring is dominated by the second order dispersion (β_2). In all the other LLE simulations, the dispersion is obtained from a fully vectorial microresonator eigenfrequency mode solver based on FEM, which includes the bending dispersion present in THz mode spacing resonators (not significant for the 100 GHz mode spacing in Fig. 4), and higher-order dispersion terms are retained. The full LLE simulation shown in Fig. 6 is performed by combining Eq. S1 with the standard LLE model, using the thermal parameters obtained in Section 1. We assume a value of the Kerr nonlinear refractive index $n_2 \approx 2.5 \times 10^{-19}$ m^2W^{-1} for Si_3N_4 [4, 5], and the effective nonlinearity γ is determined from this value and the FEM-determined effective modal area [6, 7].

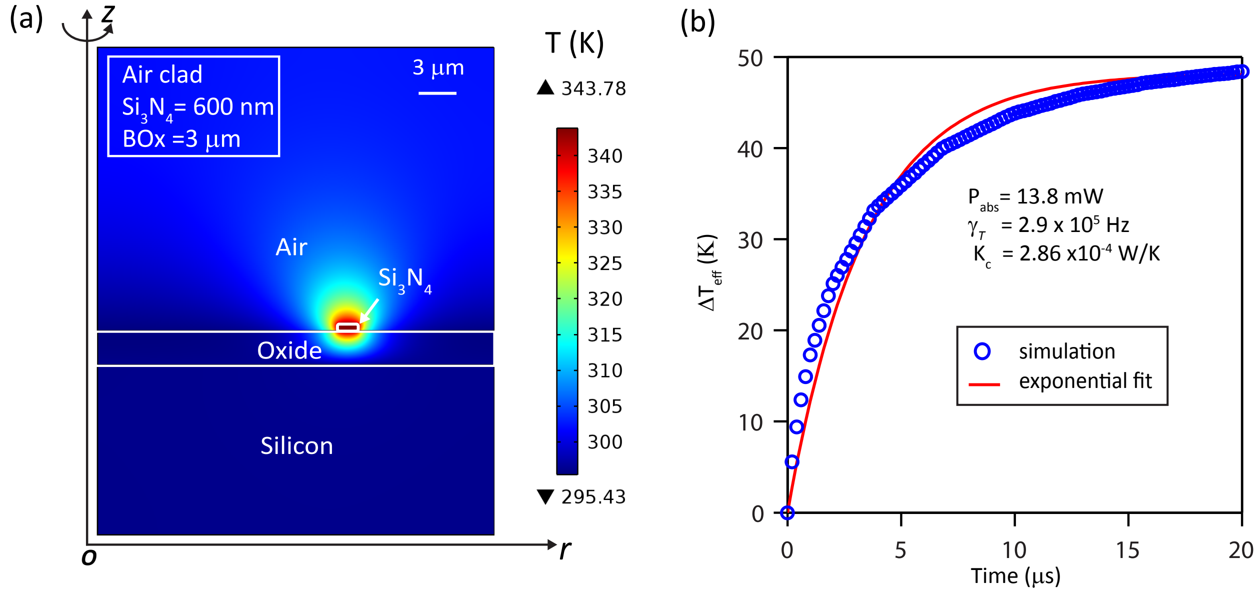

Fig. S1. Numerical simulation of the thermal properties for an air-clad Si_3N_4 microresonator. (a) Steady-state temperature distribution of a 23 μm radius Si_3N_4 microring resonator with 13.8 mW absorption power. The Si_3N_4 thickness is 600 nm and the buried oxide (BOx) layer thickness is 3 μm. (b) Simulated effective temperature T_{eff} relative to the ambient temperature (blue circles) after turning on the heat source at $t = 0$. The red solid line is the exponential fit to extract the thermal decay rate and the thermal conductance of the resonator.

Table S1. Parameters used in the LLE simulations in the main text

Figure No.	Q_c/Q_i	Dispersion	Radius(μm)	Power (mW)
4	$1 \times 10^6/1 \times 10^6$	$\beta_2 = -1.6 \times 10^{-25}$ $ps^2/(nm \cdot km)$ (From Ref. [3])	230	750
5 & 6	$6 \times 10^5/1 \times 10^6$	FEM simulation	23	40, 80 (see the legend)
8	$5 \times 10^5/2 \times 10^6$	FEM simulation	23	80

REFERENCES

1. V. Il'chenko and M. Gorodetskii, "Thermal nonlinear effects in optical whispering gallery microresonators," Laser Phys **2**, 1004–1009 (1992).
2. T. Carmon, L. Yang, and K. J. Vahala, "Dynamical thermal behavior and thermal self-stability of microcavities," Opt. Express **12**, 4742–4750 (2004).
3. H. Guo, M. Karpov, E. Lucas, A. Kordts, M. H. Pfeiffer, V. Brasch, G. Lihachev, V. E. Lobanov, M. L. Gorodetsky, and T. J. Kippenberg, "Universal dynamics and deterministic switching of dissipative Kerr solitons in optical microresonators," Nature Physics **10**, DOI: 10.1038/NPHYS3893 (2016).
4. K. Ikeda, R. E. Saperstein, N. Alic, and Y. Fainman, "Thermal and kerr nonlinear properties of plasma-deposited silicon nitride/silicon dioxide waveguides," Optics express **16**, 12987–12994 (2008).
5. J. S. Levy, A. Gondarenko, M. A. Foster, A. C. Turner-Foster, A. L. Gaeta, and M. Lipson, "Cmos-compatible multiple-wavelength oscillator for on-chip optical interconnects," Nat. Photonics **4**, 37–40 (2010).
6. Q. Lin, O. J. Painter, and G. P. Agrawal, "Nonlinear optical phenomena in silicon waveguides: modeling and applications," Optics Express **15**, 16604–16644 (2007).
7. Q. Li, M. Davanco, and K. Srinivasan, "Efficient and low-noise single-photon-level frequency conversion interfaces using silicon nanophotonics," Nat. Photonics **10**, 406–414 (2016).